

The Supplementary Materials for “Interfacial diffusion of a single cyclic polymer chain” by Shaoyong Ye, Qingquan Tang, Jingfa Yang, Ke Zhang, Jiang Zhao

1. Materials and Measurements

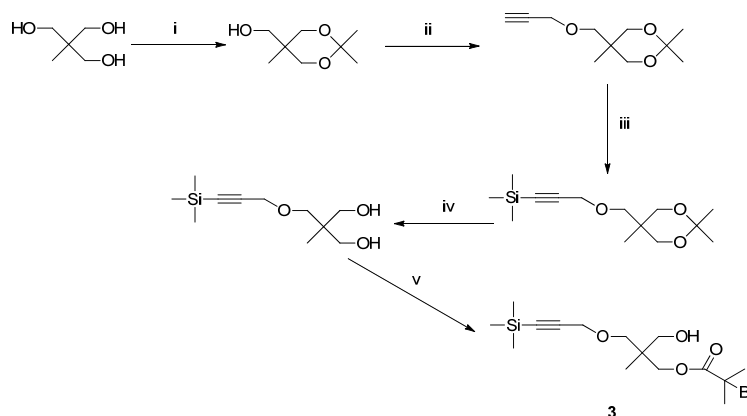
1,1,1-(trihydroxymethyl) ethane, n-butyllithium (n-BuLi, 2.2 M in hexane), trimethylchlorosilane (TMSCl), dimethyl(amino)pyridine (DMAP), DOWEX ion-exchange resin, 2-bromoisobutyryl bromide (BIB), pentamethyldiethylenetriamine (PMDETA), sodium hydride (NaH), propargyl bromide solution (~80% in toluene), anisole, sodium azide (NaN₃), 4-toluene sulfonic acid (*p*-TsOH), hydrochloric acid (HCl), tetrabutylammonium fluoride (TBAF, 1mol/L in THF), anhydrous magnesium sulfate (MgSO₄), dicyclohexylcarbodiimide (DCC), succinic anhydride, alkaline alumina (Al₂O₃), acetone, hexane, methanol, petroleum ether, ethyl acetate, diethyl ether were all purchased and used as received. Styrene (St), dichloromethane (DCM), tetrahydrofuran (THF) and *N,N*-dimethylformamide (DMF), from Aldrich, were dried and distilled prior to use. Triethylamine (TEA, Beijing Chemical Reagent Co.) was dried over KOH. Copper(I) bromide (CuBr, Alfa Aesar) was washed by acetic acid and ethanol three times respectively, and then dried under vacuum. Deionized water (18.2 MΩ·cm) was obtained by Millipore. Polystyrene gel bead (S-X1, Bio-Rad), Rhodamine 6G (R6G, Standard purity, Fluka) and Bodipy-FL (Invitrogen) were used as received without further treatment. Fused silica cover slips purchased from SPI Supplies were chosen as the model surface, used after cleaning treatments.

¹H-NMR spectra were recorded in CDCl₃ on a Bruker Avance 400MHz spectrometer, using the TMS peak for calibration. Gel permeation chromatography (GPC) was carried out on a series of four linear Styragel columns (HT2, HT3, HT4, and HT5), equipped with a Waters 1515 isocratic HPLC pump and a Waters 2414 differential refractive index detector. The eluent was THF at a flow rate of 1.0 mL·min⁻¹. Linear polystyrene standards were used for the calibration. Fourier transform infrared absorption spectra (FT-IR) were obtained on a Thermo Nicolet Avatar-330 spectrometer. The spectra were collected over 64 scans with a spectral

resolution of 4 cm^{-1} . The samples were prepared by solvent casting on a KBr plate.

2. Synthesis, characterization and fluorescence labeling of linear polystyrene (*l*-PS) and cyclic polystyrene (*c*-PS)

2.1 Synthesis and Characterization of TMS-Alkyne(Hydroxyl) ATRP Initiator 3



Scheme S1. Synthesis of TMS-alkyne (Hydroxyl) ATRP initiator (**3**). (i) Acetone, *p*-TsOH, RT, overnight; (ii) THF, NaH, propargyl bromide, 0°C , overnight; (iii) *n*-BuLi, TMSCl, THF, 0°C , 3h; (iv) DOWEX, Methanol, R.T. 24 h; (v) THF, BIB, 0°C -R.T., 16 h.

The atom transfer radical polymerization (ATRP) initiator **3** was synthesized according to the published protocols,^{1,2,3}(shown in Scheme S1). The alkyne group of initiator was intended to be protected to avoid the possible Glaser coupling. $^1\text{H-NMR}$ (400 MHz, CDCl_3) spectra and the corresponding peak assignments of the initiator were shown in Figure S1.

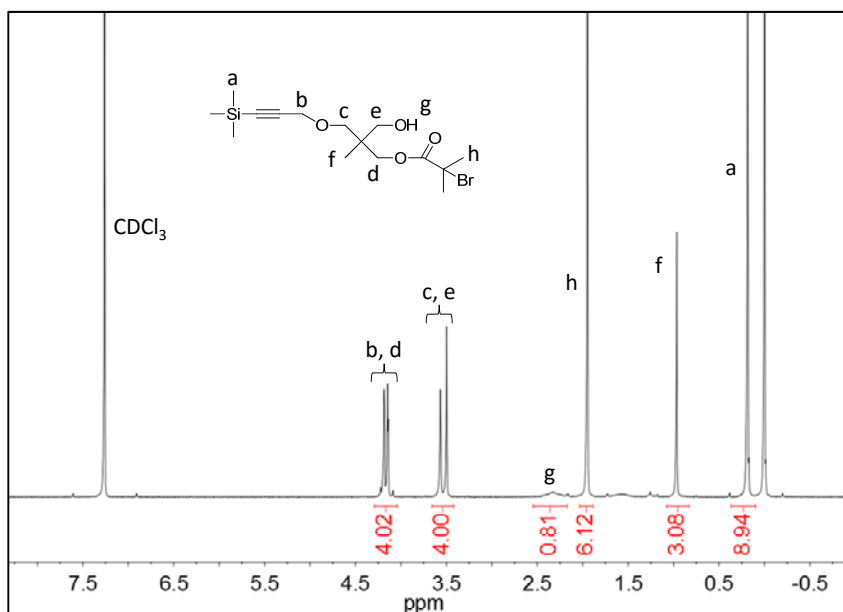


Figure S1. $^1\text{H-NMR}$ spectra of TMS-alkyne (Hydroxyl) ATRP initiator (**3**) in CDCl_3 .

2.2 Synthesis and Characterization of *l*-PS

Atom transfer radical polymerization (ATRP) was conducted under varied feed ratios to prepare *l*-PS with varied molecular weights using the ATRP initiator **3**. A typical procedure for ATRP synthesis of PS was as follows. Initiator **3**, PMDETA, St and anisole (with the same weight as St) were mixed in a 25 mL Schlenk tube. After degassing through three freeze-evacuate-thaw cycles, CuBr was added to the mixture in the frozen state under nitrogen. After three further evacuate cycles, the reaction mixture was sealed and stirred at 90°C for varied amount of time and then terminated by freezing the Schlenk tube with liquid nitrogen. Afterwards, the mixture was diluted with THF and passed through a short basic alumina column to remove the catalyst. This THF solution was concentrated and then precipitated into methanol. The same precipitation process was repeated three times to obtain pure polymer. After that, sodium azide was used to transform terminal bromine into terminal azide in DMF solution. Then, the terminal alkyne group was recovered by de-protection with TBAF in THF solution to yield the linear PS precursors **2** nominated as *l*-PS, shown in Chart 1 in the text. The obtained product was precipitated into methanol and dried overnight in a vacuum oven. The procedure for this end group modification was shown in Scheme S2. The monomer conversions were obtained from $^1\text{H-NMR}$, and the

molecular weights and molecular weight distributions were determined by GPC, as shown in Table S1 and Figure S2. Besides, molecular weights obtained from $^1\text{H-NMR}$ were plotted against those obtained from GPC to confirm the consistency of data of the two methods in Figure S3.

Table S1. Parameters for ATRP and molecular characteristics of *l*-PS.

Polymer	Monomer ^a	Feed ratio ^b	Conv. (%) ^c	M_n^d	M_w/M_n^d
<i>l</i> -PS-2.9k	Styrene	70:1:1:0.5	22.96	2860	1.04
<i>l</i> -PS-5.6k	Styrene	400:2:1:1	20.89	5590	1.03
<i>l</i> -PS-8.6k	Styrene	400:2:1:1	33.33	8590	1.04
<i>l</i> -PS-11.7k	Styrene	600:1:1:1	16.60	11680	1.05
<i>l</i> -PS-14k	Styrene	600:1:1:1	19.67	13980	1.05
<i>l</i> -PS-17.6k	Styrene	600:1:1:1	24.41	17580	1.04
<i>l</i> -PS-21.5k	Styrene	600:1:1:1	29.82	21450	1.05

^a ATRP polymerization was performed at 90°C. ^b Initial molar ratio of monomer/initiator/PMDETA/CuBr with anisole as solvent (of the same weight as St). ^c Calculated from the $^1\text{H-NMR}$ spectrum. ^d Calculated from GPC, in which THF were used as the eluent and linear polystyrene standards were used for the calibration.

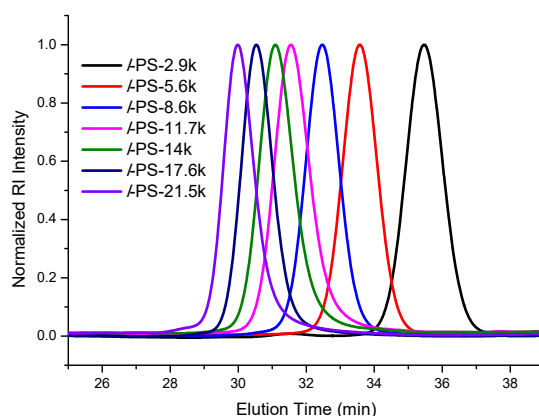


Figure S2. GPC curves of *l*-PS with varied molecular weights. THF was used as the eluent. Signals were recorded using a differential refractive index detector.

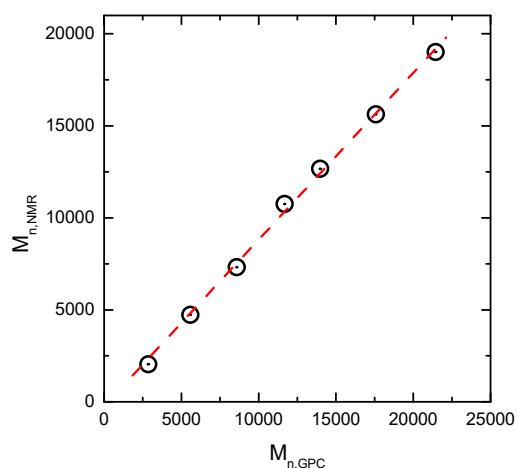
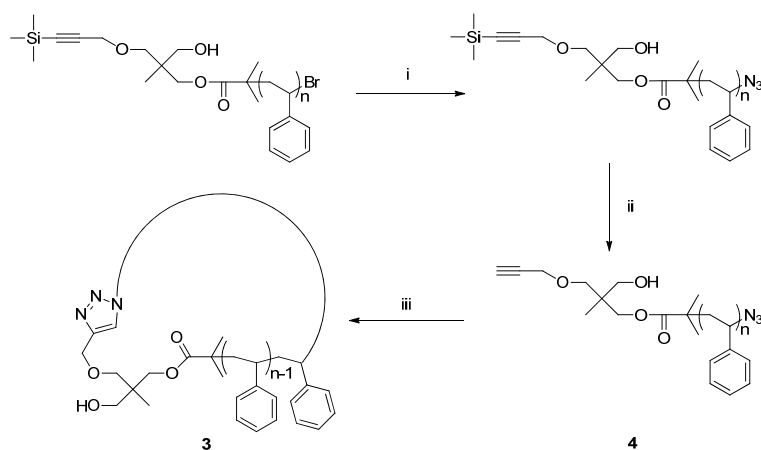


Figure S3. Molecular weights of *l*-PS measured by $^1\text{H-NMR}$ plotted against the values measured by GPC.

2.3 Synthesis and Characterization of *c*-PS

Subsequently, *c*-PS was synthesized by Cu-catalyzed azide/alkyne cyclo-addition (CuAAC) click reaction to ring-close the linear precursor **2** (*l*-PS) in a highly diluted solution via the following protocol,^{2,4,5} shown in Scheme S2. PMDETA, dissolved in 230 mL of DMF, was added into a 250 mL Schlenk tube. After purging with nitrogen for 1 h, the solution was introduced into a 1 L Schlenk tube containing CuBr and stirred at 50°C for 30 min to allow the formation of CuBr/PMDETA complex. A separate 500 mL Schlenk tube containing 450 mL polymer solution was de-oxygenated by the same way and then slowly added into the 1 L Schlenk tube under the protection of nitrogen flow, with a 50 times molar excess of CuBr and PMDETA to polymer.⁶ The final concentration of cyclization solution was kept at about 10^{-5} M to reduce intermolecular couplings to the greatest extent. Then, the reaction mixture was stirred vigorously for 24 h or more at 50°C to ensure the completion of intra-molecular cyclization. After that, DMF was removed under reduced pressure, and the solid mixture was re-dissolved in DCM and passed through a neutral alumina column to remove the catalyst. The DCM solution was concentrated and then precipitated into methanol. After drying the solid product, multiple fractionations were adopted to obtain highly purified cyclic PS **1** (*c*-PS), shown in Chart 1 in the text.



Scheme S2. Synthesis of *l*-PS and *c*-PS. (i) NaN₃, DMF, 40°C, 48h; (ii) (C₄H₉)₄NF, THF, R.T. 24 h; (iii) Cu(I)Br, PMDETA, DMF, N₂, 40°C, 24h.

In Figure S4(a), the overlapped GPC curves of *c*-PS with ring-closure reaction time of 5.5h, 10.0 h and 11.0 h evidence the completion of the ring-closing reaction even within the shortest reaction time (5.5h), consistent with the very fast reaction nature, i.e. 8 min, of CuAAC for this polymer system reported previously.⁶ Nevertheless, we extended our ring-closure reaction time to about 24 h or even 48 h to ensure the complete ring-closure of linear precursors. The completion was also evidenced by the disappearance of azide peak at 2100 cm⁻¹ in the FT-IR spectra of *c*-PS, as compared with that of *l*-PS in Figure S5. Figure S4(b) displays the results of *c*-PS with multiple fractionation conduction, demonstrating that the high molecular weight impurities can be removed to a large extent. Note that the fractionation procedure is not necessary for molecular weights lower than 10 kg·mol⁻¹ because the high efficiency of CuAAC is sufficient to lead to the well-defined, mono-modal, and symmetrically shifted GPC curves for *c*-PS. Figure S6 showed GPC curves of *l*-PS (black) and the resultant *c*-PS (red) with seven different molecular weights. For *c*-PS-2.9k, *c*-PS-5.6k and *c*-PS-8.6k, the GPC curves were obtained without purification.

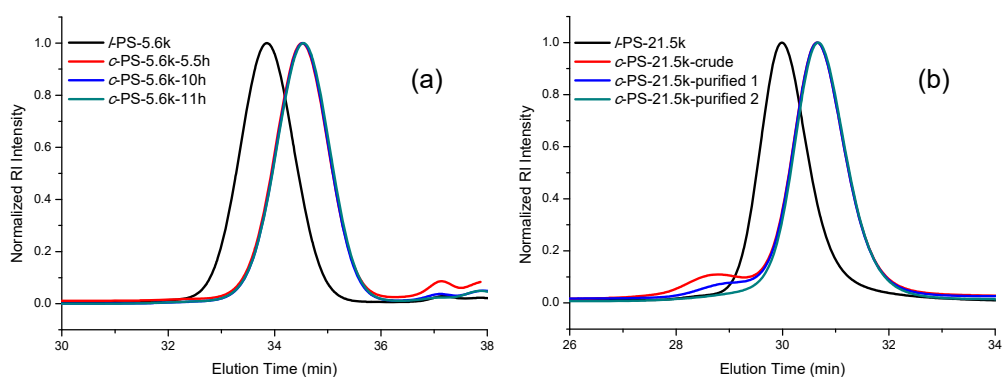


Figure S4. (a) GPC curves of *c*-PS with different ring-closure reaction time for linear precursor *l*-PS-5.6k (black); (b) GPC curves of *c*-PS with molecular weight 21.5k g·mol⁻¹ before and after fractionations with linear precursor as the reference.

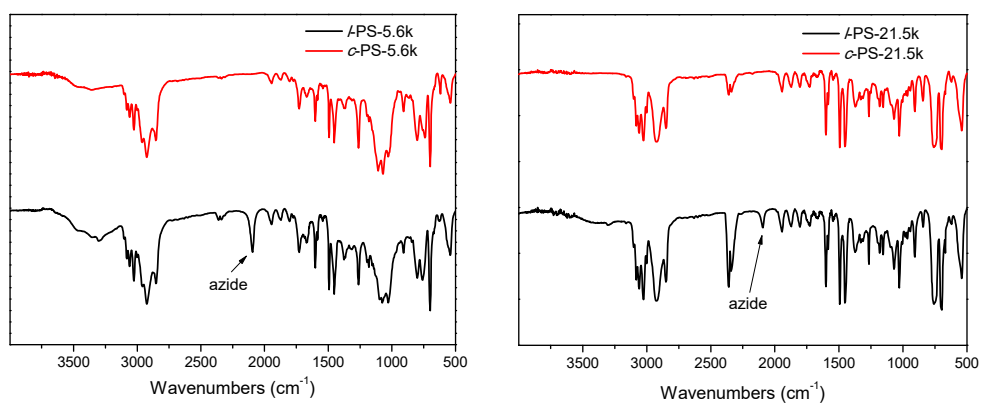


Figure S5. FT-IR spectra obtained for *l*-PS (black) and the resultant *c*-PS (red).

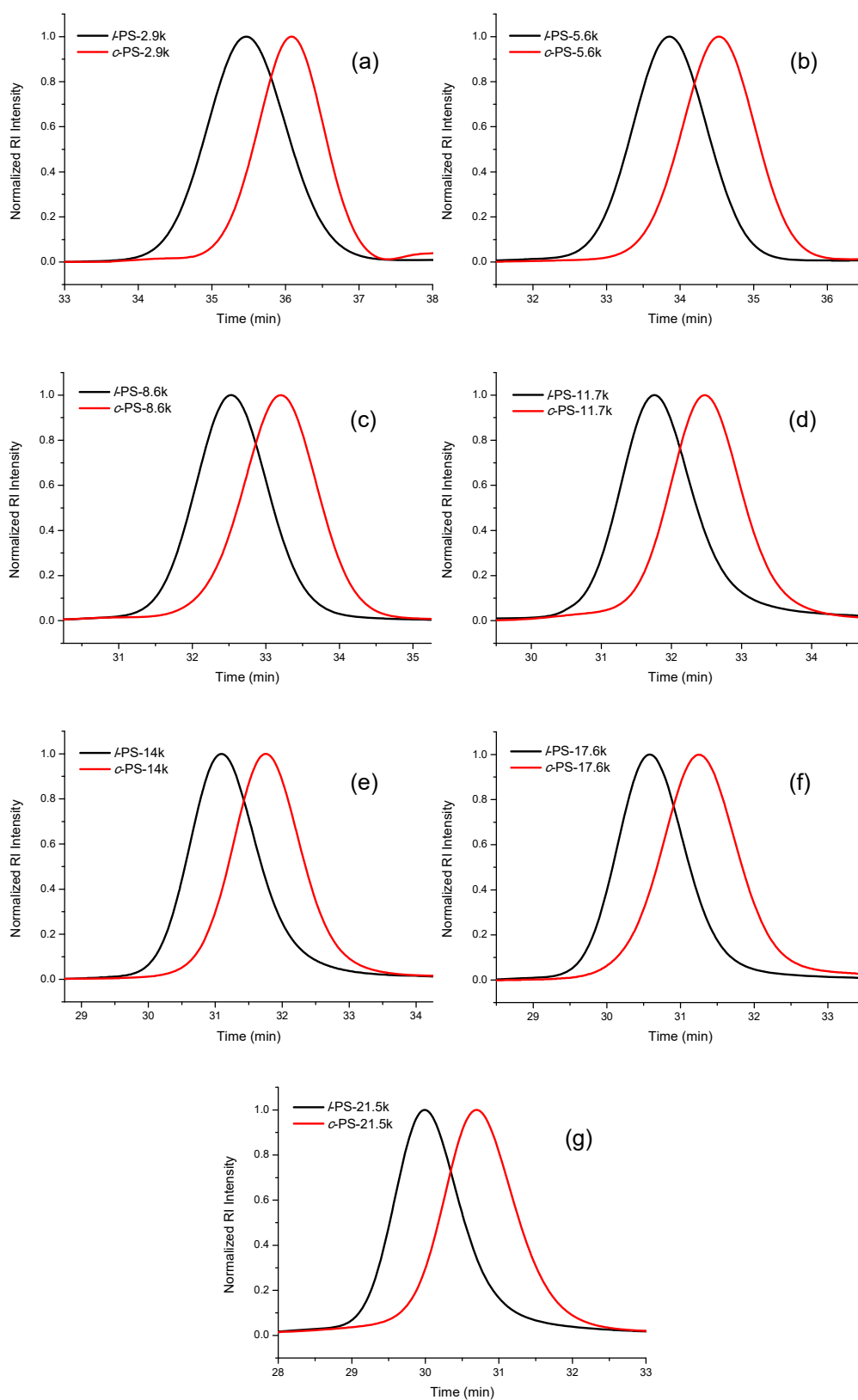


Figure S6. GPC curves of *l*-PS (black) and the resultant *c*-PS (red) with seven different molecular weights. (a) 2.9k g·mol⁻¹; (b) 5.6k g·mol⁻¹; (c) 8.6k g·mol⁻¹; (d) 11.7k g·mol⁻¹; (e) 14k g·mol⁻¹; (f) 17.6k g·mol⁻¹; (g) 21.5k g·mol⁻¹.

Both diffusion of a single fluorescence-labeled PS chain on mechanically polished fused silica and in solution was investigated by fluorescence correlation spectroscopy (FCS). The excitation laser beam was tightly focused into the sample through the objective lens. The fluorescence from the sample was collected by the same objective and the intensity fluctuation caused by fluorescent species diffusing in and out of the tiny excitation-detection volume, was recorded by single photon counting modules. The generation of correlation function was conducted by the integrated electronic hardware and the relevant software. By numerical fitting using two-dimensional or three-dimensional Brownian motion models, the value of diffusion coefficient and the average concentration of the labeled molecules are obtained. The explicit descriptions of FCS principles can be found in a number of publications.⁸⁻¹⁰

Experiments were performed on a home-built one-photon FCS set-up.^{7,11,12} It was based on an inverted microscope (Olympus IX-71). The excitation laser was the 488 nm output of a solid laser (Exxon, Germany) and it was introduced into the microscope and focused into the sample through a water-immersion objective (UPlanApo 60×, number aperture = 1.20, working distance = 0.25 mm) with its correction collar ring fixed at 0.16 mm in order to be compatible with the thickness of the coverslips. The fluctuation in the fluorescence signal was measured respectively by two photomultiplier tube-based single photon counting modules (Hamamatsu). Data acquisition and auto-correlation function analysis was conducted by a commercial FCS board and its software (ISS Inc.).

The power density of the excitation laser was kept low to prevent possible artifacts by heating and potential photo-degradation and the typical intensity of $4.6 \times 10^7 \text{ W} \cdot \text{m}^{-2}$ ($\sim 10 \text{ } \mu\text{W}$ at the sample stage) was used. This value is quite low, about 6 times lower than the reported values for the identical physical system.^{13,14} For the solution measurements, the labeled PS samples were dissolved in DCM at a concentration of $\sim 10^{-9} \text{ M}$. The typical FCS curves were shown in Figure 1(a) for a few cyclic samples. The expression of the autocorrelation function by the three-dimensional Gaussian

model is $G(\tau) = \left(\pi^{\frac{3}{2}} w_0^2 z_0 \langle c \rangle \right)^{-1} \left(1 + \frac{4D\tau}{w_0^2} \right)^{-1} \left(1 + \frac{4D\tau}{z_0^2} \right)^{-\frac{1}{2}}$, where w_0 and z_0 are the lateral radius and the half length of the excitation-detection volume, respectively. The dimension of the excitation-detection volume was calibrated by measuring diffusion of the standard substance, Rhodamine 6G, and the lateral radius and vertical half length of the confocal volume was determined to be 260 nm and 1.5 μm for 488 nm laser. Figure S7 displays the data collected in solution and the fitting results for PS with lower molecular weights in dilute DCM solution, consistent with the ideal random coil conformation with hydrodynamic interactions found in many neutral polymer systems in good solvents.

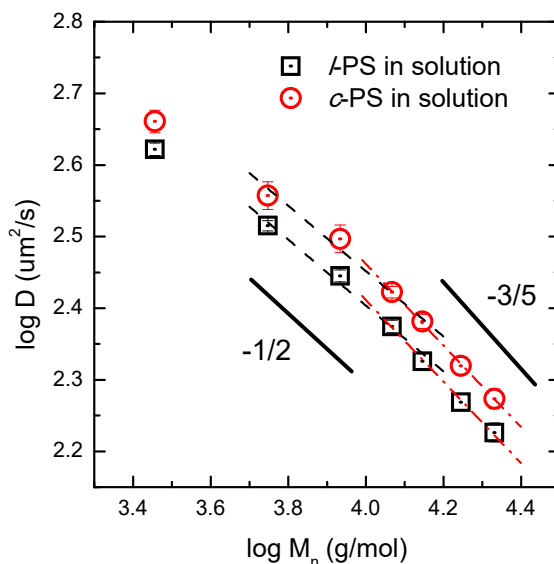


Figure S7. Double-logarithmic plots of center-of-mass diffusion coefficient (D) against molecular weight (M) for cyclic (red circles) and linear (black squares) polystyrene chains in dilute dichloromethane solution. The solid lines with slopes $-1/2$ and $-3/5$ are drawn as guides to the eye. The dashed lines through the points representing the best fits of the data give the power-law slope -0.46 ± 0.03 for linear chains and -0.46 ± 0.05 for cyclic chains, respectively. The power-law slopes of the dashed-dotted lines are given in the text.

3.2 Surface Diffusion Measurements

In order to conduct single-molecule surface diffusion measurements, the cleaning treatments for model substrates are necessary. The substrates, i.e. fused silica coverslips (SPI Supplies), were immersed in Piranha solution (a mixture of

concentrated sulfuric acid and hydrogen peroxide) at 100°C for ~1h. The substrates were then rinsed thoroughly with deionized water and dried under nitrogen flow. Treatment under oxygen plasma was performed for 1.0 h to guarantee the complete removal of fluorescent contaminants. Finally, the substrate was mounted in the home-built sample cell¹⁵, which is well-sealed.

Fluorescence-labeled PS was dissolved in its good solvent, DCM. To begin the surface diffusion measurements, the polymer chains were allowed to adsorb onto the surface of fused silica quartz coverslips from dilute (10^{-9} M) DCM solution for 5.0 min, followed by vigorous rinsing with pure solvent at least 10 times to remove un-adsorbed polymers in solution. The focus of the laser beam was carefully adjusted onto the silica surface to conduct lateral diffusion measurements of adsorbed labeled polymer chain.¹² The lateral diffusion coefficient and the number of fluorescence molecules inside the excitation surface plane were obtained by fitting the obtained autocorrelation curves with a two-dimensional Brownian motion model, as shown in Figure 1(b) in the text. The expression of the autocorrelation function by the two-dimensional Gaussian model is $G(\tau) = \frac{1}{\pi w_0^2 \langle \rho \rangle} \left(1 + \frac{4D\tau}{w_0^2} \right)^{-1}$, where w_0 is the lateral radius of the excitation-detection volume.

Diffusion coefficient of each PS sample presented in the text was the average of 10-20 separate measurements performed on different surface locations of the same substrate or repeated on other new freshly-made ones and the error bars show the standard deviation, also illustrated in the Figure S8. The surface concentration of probe chains was about 5-10 molecules· μm^{-2} , indicating a large average inter-molecular distance of at least over 200 nm. This condition corresponds to the situation of the isolated chain on surface without interference of polymer-polymer interactions. Control experiments show that the fluorescence molecule chosen in this study does not adsorb onto the substrate.¹³ All FCS experiments were conducted at room temperature, 23-25°C. Figure S9 displays the whole data collection for PS samples diffusing in dilute solution and on solid surface and the best fitting results.

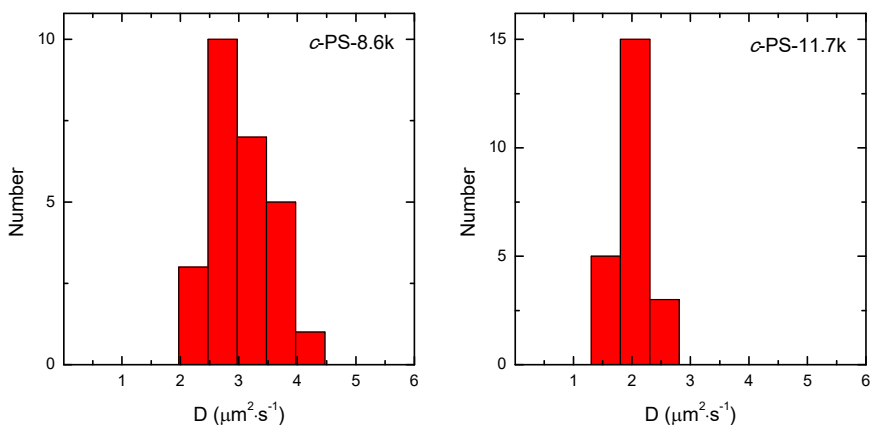


Figure S8. Histograms of surface diffusion coefficients obtained for *c*-PS-8.6k and *c*-PS-11.7k.

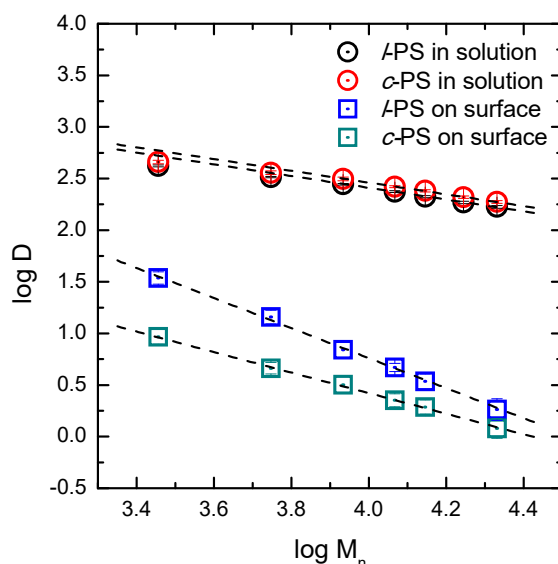


Figure S9. Double-logarithmic plots of center-of-mass diffusion coefficient (D) against molecular weight (M) for surface diffusion of cyclic (circles) and linear (squares) polystyrene chains on fused silica-dichloromethane interface compared with diffusion in dilute dichloromethane solution. The error bars are the standard deviation averaging about 10-20 individual experiments and of the size of the symbols. The dashed lines through the data with slopes are the best fitting results.

3.3 Prediction on the convergence of scaling laws at high molecular weight

An intersection point between the two data sets of *l*-PS and *c*-PS is predicted in high molecular region, by extrapolation of the two data sets. It is anticipated that the two data sets will converge to an identical set with the same scaling law, i.e. the Rouse dynamics, as shown in Figure S10. The crossover of dark red solid lines denotes the transition point from the reptation to Rouse dynamics referring to the literature.¹³As

can be seen, molecular weight of the intersection point obtained for cyclic and linear PS in the current work is close to that of the transition point found for linear PS samples in a previous study, partially confirming our argument.¹³

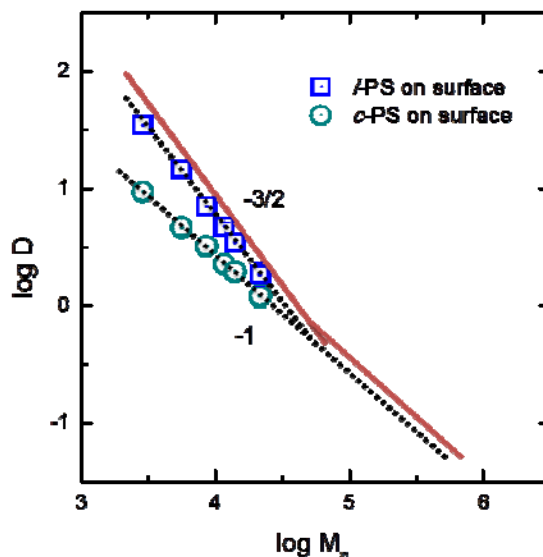


Figure S10. Double-logarithmic plots of center-of-mass diffusion coefficient (D) against molecular weight (M) for surface diffusion of cyclic (circles) and linear (squares) polystyrene chains on fused silica-dichloromethane interface compared with the trend of the scaling law transition referring to the literature (dark red solid lines). The dotted lines through the data denote the existence of the intersection point located in the high molecular weight range, which is very close to the transition point for linear polystyrene in this specific physical system.¹³

References

1. Z. Jia, D. E. Lonsdale, J. Kulis and M. J. Monteiro, *ACS Macro Lett.* 2012, **1**, 780-783.
2. D. M. Eugene and S. M. Grayson, *Macromolecules* 2008, **41**, 5082-5084.
3. M. D. Hossain, Z. F. Jia and M. J. Monteiro, *Macromolecules* 2014, **47**, 4955-4970.
4. J. Ye, J. Xu, J. Hu, X. Wang, G. Zhang, S. Liu and C. Wu, *Macromolecules* 2008, **41**, 4416-4422.
5. B. A. Laurent and S. M. Grayson, *J. Am. Chem. Soc.* 2006, **128**, 4238-4239.
6. D. E. Lonsdale, C. A. Bell and M. J. Monteiro, *Macromolecules* 2010, **43**, 3331-3339.

7. S. J. Luo, X. B. Jiang, L. Zou, F. Wang, J. F. Yang, Y. M. Chen and J. Zhao, *Macromolecules* 2013, **46**, 3132-3136.
8. D. Magde, E. Elson and W. W. Webb, *Phys. Rev. Lett.* 1972, **29**, 705-708.
9. R. Rigler and J. Widengren, *BioScience* 1990, **3**, 180.
10. E. Elson and D. Magde, *Biopolymers* 1974, **13**, 1-27.
11. S. Q. Wang and J. Zhao, *J. Chem. Phys.* 2007, **126**, 091104.
12. Q. B. Yang and J. Zhao, *Langmuir* 2011, **27**, 11757-11760.
13. J. S. S. Wong, L. Hong, S. C. Bae and S. Granick, *Macromolecules* 2011, **44**, 3073-3076.
14. S. A. Sukhishvili, Y. Chen, J. D. Müller, E. Gratton, K. S. Schweizer and S. Granick, *Macromolecules* 2002, **35**, 1776-1784.
15. J. Zhao and S. Granick, *Macromolecules* 2003, **36**, 5443-5446.